Submission to J. Environm. Radioactivity

Simulating uranium sorption onto inorganic particles: the effect of redox potential

Abstract

An analytical expression is proposed to simulate the effects of pH and redox potential (*E*) on the sorption of uranium onto model inorganic particles in aquatic environments instead of following an experimental approach providing a list of empirical sorption data. The expression provides a distribution coefficient (*Kd*) as function of pH, *E* and ligand concentration (complex formation) applying a surface complexation model on one type of surface sites (>SuOH). The formulation makes use of the complexation and hydrolysis constants for all species in solution and those sorbed at the surface, using correlations between hydrolysis constants and surface complexation constants, for the specific sorption sites. The model was applied for the sorption of uranium onto aluminol, iron hydroxide and silanol sites, mimicking respectively 'clean' clay or 'dirty' clay and 'clean' sand or 'dirty' sand ('dirty' referring to iron hydroxide contaminated), in absence or presence of carbonates in solution. The calculated distribution coefficients are very sensitive with the presence or absence of carbonates. The *Kd* values obtained by applying the model are compared with values reported in the literature for the sorption of uranium onto specific adsorbents. It is known that in surface water, U(VI) and its

hydroxides are the primary stable species usually observed. However, reduction to U(IV) is possible and may be simulated during sorption or when the redox potential (*E*) decreases. Similar simulations are also applicable to study the sorption of other redox sensitive elements.

Keywords: *uranium sorption, redox potential, surface complexation, distribution coefficient*

Graphical abstract

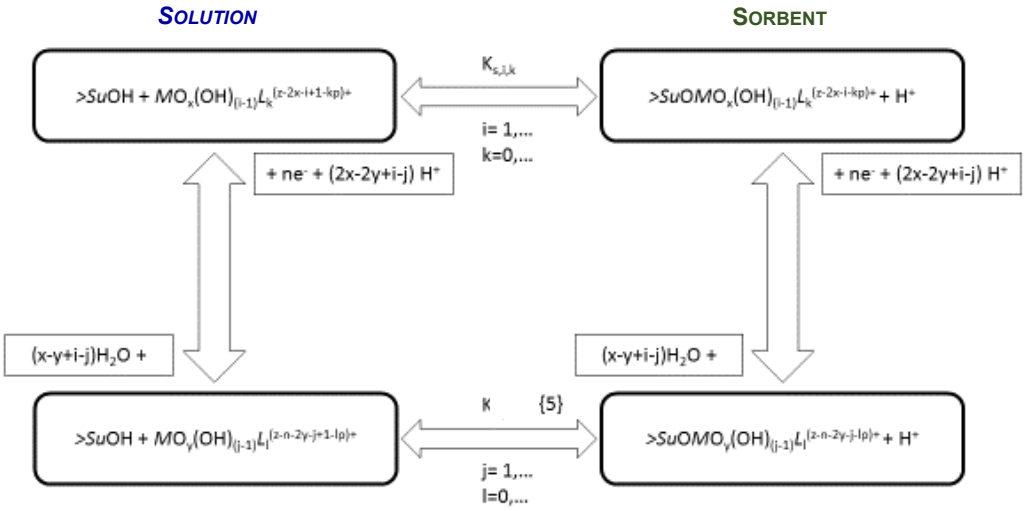

Reactions in *SOLUTION* and at the SORBENT interface that must be considered to derive the model as Kd = f(pH,*E*,[L],*d*,{>SuOH},*Δ*) for the redox couple $M^{z+}/M(^{z-n)+}$, with ions complexed by hydroxyl (OH^-) and ligand (L) onto surface sorbing group (>*Su*OH) of density *Δ* on particles of size *d* at a given pH and for redox potentials *E*.

1. Introduction

Issues associated with the environmental behaviour of uranium has been the topic of numerous studies e.g. Selvakumar et al (2018); Gavrilescu et al (2008). The release of uranium from a contaminated sediment and its local retention are governed by biochemical reactions including factors such as acidity, redox potential, presence of ligand (inorganic, organic and bioorganic) of the water e.g. Ulrich et al (2009). The sorption of uranium on specific sediment components is consequently a relevant issue to investigate.

The sorption of actinides onto selected inorganic model alumina and goethite colloidal particles has already been reported by Degueldre *et al.* (1994) and by Ulrich *et al*. (2006). Recently specific studies were also carried out on magnetite (Fe_3O_4) by Singhal *et al*. (2017), on titanium oxide (TiO_2) by Lefèvre *et al* (2008) and by Li *et al*. (2019), on zircon by Lomenech *et al*. (2003), on clayeous materials such as smectite by Chisholm-Brause *et al*. (2004), muscovite by Richter *et al.* (2016) and zeolite ($Na_2Al_2Si_3O_{10}.2H_2O$) by Su *et al*. (2018). Most of these sorption studies are **empirical** and a formal approach of distribution coefficient (*Kd*) determination is missing.

In sorption studies, analytical expressions based on the relation of the distribution coefficient (*Kd*) and the thermodynamic properties of the phases has been applied since the formula derived in the pioneered work of Degueldre *et al*. (1994). The sorption includes surface complexation with one type of sorbent surface site (>SuOH). The model has been completed for redox effects considering the redox potential in solution for all hydrolysed species in solution and on the surface. Complexation with ligands was also included in the formulation as

carbonate, or total inorganic carbon (TIC), which is expected to affect significantly the speciation and the sorption of metal ions in waters at quasi neutral pH values. The sorption of metal ions onto particles is affected by many parameters such as pH, redox potential (*E*), sometime called *Eh*, ligands concentration, e.g. [TIC], or sorption kinetics. The influence of pH in sorption is well established, but the effort made in studying the influence of redox potential is limited, as reported for other actinide elements e.g. Degueldre & Bolek (2009).

The study of the redox potential effect in the sorption is especially relevant in environmental science. However, it can be difficult to study the effect experimentally (Grenthe *et al,* (1992)). Fortunately, solutions (e.g. working electrode in-line polishing) have been suggested by Degueldre *et al.* (1999).

The objective of this study is to calculate the distribution coefficient as a function of pH, redox potential concentration of ligand and nature of the sorbent. This approach has been applied to the sorption of uranium, a redox sensitive actinide, onto three selected inorganic model particles (Al_2O_3, FeOOH and SiO_2). These model particles could mimic clean clay (Al_2O_3), 'dirty' clay or sand (surface contamination with FeOOH) and clean sand (SiO_2) some key components of the terrestrial environment. Organic material shall be considered in a separate study.

The ultimate aim of this work is to develop a more multipurpose model of material sorption, as part of the strategy suggested by Degueldre *et al.* (2019) to upgrade the nuclear fuel cycle through regenerative extraction of uranium to become a renewable resource.

2. Modelling species occurrence and their sorption properties

89 The sorption process involves reactions ranging from 'inner sphere' complex formation with
90 active surface sites to ion exchange. It is usually described by the distribution ratio, which at
91 equilibrium yields a distribution coefficient (*Kd*) as given by Equation (1):

92 $$Kd = \frac{[M]_{sorbed}}{[M]_{solution}} \frac{1}{[part]} \quad (1)$$

93 where [*part*] is the particle concentration (e.g. in g·mL^{-1}) and [*M*] is the concentration of the
94 element sorbed on the particles or present in solution (both in: mmol·mL^{-1}). The inclusion of
95 [*part*] in this ratio is intended to generalise the more classical distribution coefficient
96 formulation: $Kd = C(\mathrm{M})_{\mathrm{part}}/[\mathrm{M}]_{\mathrm{sol}}$ (with $C(\mathrm{M})_{\mathrm{part}}$ in mmol.g^{-1}) to one where the sorbent is in the
97 liquid matrix (suspension).
98
99 **2.1 Particles and sorption sites**
100
101 In this work metal ions e.g. $\mathrm{M(OH)_i^{(z-i)+}}$ are sorbed onto monodentate sites >SuOH, where Su
102 represents the substrate material available at the surface of particles (part). The distribution
103 coefficient in a Langmuir model is directly proportional to [>SuOH]/[*part*], with [>SuOH] the
104 site concentration (e.g. mol mL^{-1}). In a simplified approach, if the particles are supposed to be
105 spherical and monodispersed, the volume of one particle is given by $V = (4/3)\ \pi\ r^3$ with *r* the
106 particle radius (cm or nm according to context). The particle mass (*M*) is consequently given by
107 $M = \rho\ V$ with ρ the density of the particle material and the number of particle per volume unit
108 (*N*) is given by $N = [part]/M$. The particle surface (*S*) is given by $S = 4\ \pi\ r^2$ and if the particle
109 surface is covered homogeneously by sites with the density Δ given in nm^{-2}. The number of
110 site per particle (n_s) can be defined as and be easily calculated as $n_s = \Delta\ S$. From this, the
111 number of site per suspension volume $N_{sv} = n_s\ N$ and consequently [>SuOH] = $\Delta\ S\ N/\mathrm{N_{Av}}$
112 where $\mathrm{N_{Av}}$ is the Avogadro constant.
113 This allows the [>SuOH]/[*part*] ratio to be evaluated as [>SuOH]/[*part*] = $3\ \Delta\ \mathrm{N_{Av}}\ /(\rho\ r)$.

The [>SuOH]/[*part*] ratio may also be derived experimentally using the specific surface provided by BET measurements. The specific surface is given by $3/\rho\, r$ in the case of ideal spherical particles. This value may be affected by the particle porosity and the fractal of its interface.

2.2 Impact of site reactivity

Protonation and deprotonation of the >SuOH sites could modify the sorption properties. These specific reactions {1} and {2} can be written:

$$>SuOH_2^+ \quad \Leftrightarrow \quad >SuOH + H^+ \qquad \{1\}$$

$$>SuOH \quad \Leftrightarrow \quad >SuO^- + H^+ \qquad \{2\}$$

The acid/base constants (K_{ai}) associated to the sites are:

$$K_{a1} = \frac{[>SuOH][H^+]}{[>SuOH_2^+]} \qquad (2) \qquad \text{and} \qquad K_{a2} = \frac{[>SuO^-][H^+]}{[>SuOH]} \qquad (3)$$

The total site concentration equals:

$$[>SuOH]_{Tot} = [>SuOH_2^+] + [>SuOH] + [>SuO^-] \qquad (4)$$

which gives:

$$[>SuOH] = \frac{[>SuOH]_{Tot}}{([H^+]/K_{a1} + 1 + K_{a2}/[H^+])} \qquad (5)$$

Further to these protonation/deprotonation reactions, leaching effects due to dissolution of the structure become significant at pH around the respective pK_a values. The reactions follow the hydrolysis then deprotonations series:

$$>Su^+ + H_2O \;\Leftrightarrow\; >SuOH_2^+ \overset{H^+}{\Leftrightarrow} >SuOH \overset{H^+}{\Leftrightarrow} >SuO^- \qquad \{3\}$$

In reality, these effects are limited by solubility of Su in water e.g. with the soluble forms of $>Su^+$ and of $>SuO^-$. Consequently the reactivity of >SuOH sites is accounted below.

2.3 Complexes formation in the redox range

The methodology follow the approach suggested earlier e.g. Degueldre (1997). The hydrolysis stability constants of both redox species ($K_{i,k}$ for oxidising and $K_{j,l}$ for reducing species) can be obtained on the basis of the stepwise reactions {4} and {5}. This notation is intended to include both oxo and non-oxocation species. Metal complexation reactions involving *k*-ligands or *l*-ligands (L^{-p}) (e.g. carbonates) were also considered. The limits on all indices are fixed by the co-ordination properties of the appropriate element.

$$MO_x(OH)_{(i-1)}L_k^{(z-2x-i+1-kp)} + H_2O \underset{\substack{i=1,...\\k=0,...}}{\overset{K_{i,k}}{\Leftrightarrow}} MO_x(OH)_i L_k^{(z-2x-i-kp)} + H^+ \quad \{4\}$$

$$MO_y(OH)_{(j-1)}L_l^{(z-2y-n-j+1-lp)} + H_2O \underset{\substack{j=1,...\\l=0,...}}{\overset{K_{j,l}}{\Leftrightarrow}} MO_y(OH)_j L_l^{(z-2y-n-j-lp)} + H^+ \quad \{5\}$$

The redox couple $MO_x^{(z-2x)+}/MO_y^{(z-n-2y)+}$ reaction (where $MO_x^{(z-2x)+}$ is the oxidised species and $MO_y^{(z-n-2y)+}$ the reduced one), is described according to reaction {6}.

$$MO_x^{(z-2x)+} + ne^- + (2x\text{-}2y)H^+ \quad \Leftrightarrow \quad MO_y^{(z-n-2y)+} + (x\text{-}y)\,H_2O \qquad \{6\}$$

The surface complexation for the hydrolysed (and complexed) species is described (reactions {4} and {5}) considering the neutral sites >*Su*OH. The surface complexation constants are $K_{s,i,k}$ for the oxidising species and $K_{s,j,l}$ for the reducing species. Their values are estimated by correlation with the hydroxo-complex constants (see Section 3.2) using a simple linear relationship:

$$.\log K_{s,i} = A + B \log K_i \qquad (6)$$

With A and B site specific constants. The indices *k* and *l* refer to the appropriate co-ordination number of the metal ions with the selected ligand. Effects of the redox potential in water and at the surface are also taken into account (reactions {7} and {8}).

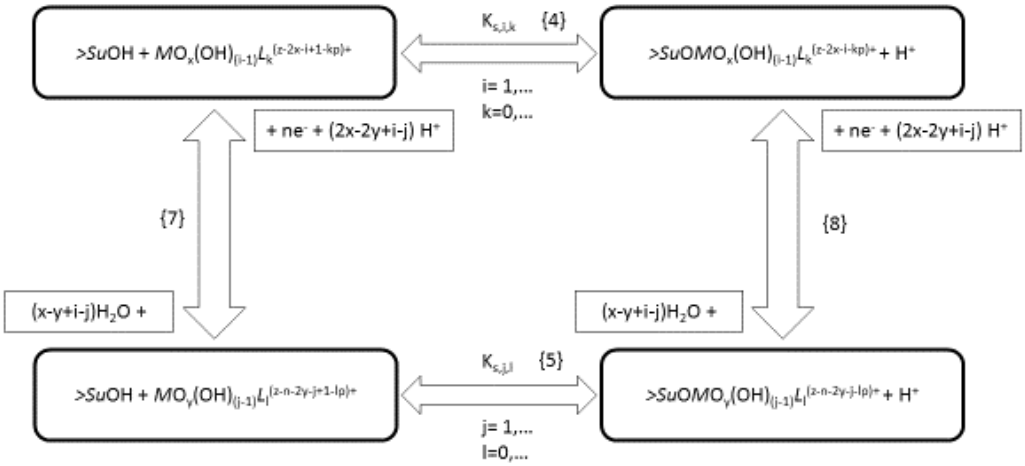

When the reactions are written in terms of free metal M^{z+}, the cumulative constants (hydrolysis) are β_i and β_j respectively ($\beta_i = \Pi K_i$).

The ratio between the concentrations of both redox species can be written as a function of the redox potential (E) applying the Nernst equation (2) for Reaction {7}.

$$E = E° + (2x\text{-}2y + i - j)\cdot RT\cdot(nF)^{-1} \ln [H^+] + RT\cdot(nF)^{-1}\ln\{[MO_x^{(z-2x)+}]\cdot[MO_y^{(z-n-2y)+}]^{-1}\} \quad (7)$$

where the standard apparent redox potential is $E'° = E° + (2x\text{-}2y + i - j)\cdot RT\cdot(nF)^{-1}\ln [H^+]$ in water . A similar apparent redox potential at the sorbent/water interface E'° may be defined for Reaction {8}.

The *Kd,* considering surface complexation and including complexation with ligands as formulated in the above-mentioned equations and reactions, can be written in terms of the redox potential (Eq. 7).

$$K_d = \frac{\{\sum_{i,k}[\frac{K_{s,i,k}\cdot\beta_{i,k}\cdot[L_k]^k}{[H^+]^i}] + \sum_{j,l}\left[\frac{K_{s,j,l}\cdot\beta_{j,l}\cdot[L_l]^l}{[H^+]^j}\right]\exp(A)\}\cdot\frac{[>SuOH]}{[H^+]}}{\{\sum_{i,k}[\frac{\beta_{i,k}\cdot[L_k]^k}{[H^+]^i}] + \sum_{j,l}[\frac{\beta_{j,l}\cdot[L_l]^l}{[H^+]^j}]\cdot\exp(A)} \quad \textbf{[part]}$$

(8)

where $A = \frac{\left(E'^{o} - E\right) \cdot n\mathrm{F}}{\mathrm{R}T}$ and [>*Su*OH] is the free site concentration that can be expressed in terms of the total surface site concentration $[>Su\mathrm{OH}]_T$ and the (de)protonation acid dissociation constants. The free ligand concentration [L] also has to be written in terms of the total ligand concentration.

The formulation (i.e. Eq. 8) implies linear adsorption isotherms and no saturation effects. No electrostatic effects and no activity corrections were considered at this stage.

3. Simulation results for uranium speciation and sorption onto particles.

3.1 Revisiting uranium speciation in solution

Prior sorption modelling, it is necessary to perform speciation modelling before to draw the uranium pH – *E* diagrams without and with carbonate.

The diagrams are drawn considering all the possible redox couples of U, namely, U(III)/U(IV), U(III)/U(V) and U(III)/U(VI), see Silva *et al*., (1995). In Table 1 the standard redox potentials reported for these redox couples (Katz *et al.* (1986), actualized OECD (2001)) are presented. The diagram calculation requires the stability constants of hydroxo species which are given in Table 2. Analytical domains are calculated using the data from Table 1 and 2, and an Excel spreadsheet software. Figure 1a presents the uranium pH – *E* diagrams calculated for a uranium concentration of 1 nM without carbonate (< 10^{-8} M CO_3 total) showing the stability domain of U(IV) and U(VI) in water stability region. The hydroxo- complexes are namely the mono-, di- and tri- hydroxo complexes for U(VI) and the mono-, di-, tri- and tetra-hydroxo complexes for U(IV). It is well established that the regions in which the pentavalent oxidation state of U has

been proposed as a significant species are at pH<5. However, no hydrolysis of UO_2^+ would be expected under these conditions.

Table 1: Standard redox potentials ($E°$) for uranium, as recommended by OECD (2001) [20], Vs SHE. In **bold** data used in this study.

Redox Couple	***E*° / V**
UO_2^{2+}/UO_2^+	0.0878 ± 0.0013
UO_2^{2+}/U^{4+}	0.2673 ± 0.0012
UO_2^+/U^{4+}	0.0447
UO_2^+/ U^{3+}	**0.053**
U^{4+}/U^{3+}	**-0.553 ± 0.004**
UO_2^{2+}/ U^{3+}	**0.006**

Table 2: Equilibrium constants for the hydrolysis of uranium species $[M^{+z}O_x](OH)_i^{(z-2x-i)+}$ for U(III), U(IV), U (V) and U(VI). Note: the values are given for infinite dilution.

	$logK_{VI, i, 0}$	**$logK_{V, i, 0}$**	**$logK_{IV, I, 0}$**	**$logK_{III, i, 0}$**
$logK_{X\ i\ 0}$	$[UO_2(OH)_i]^{(2-i)+}$	$[UO_2(OH)_i]^{(1-i)+}$	$[U(OH)_i]^{(4-i)+}$	$[U(OH)_i]^{(3-i)+}$
$LogK_{X, 1, 0}$	-5.25 ± 0.500 [b]	-11.30 [b]	-0.54 ± 0.060 [a]	-6.80 ± 0.300 [b]
$LogK_{X, 2, 0}$	-6.9 [b]	-12.30 [b]	-0.70 [a]	-7.30 [b]
$LogK_{X, 3, 0}$	-8.10 [b]		-3.60 [a]	-11.60 [b]
$LogK_{X, 4, 0}$	-12.15 [b]		-5.3 ± 0.500 [a]	-14.35 [b]
$LogK_{X, 5, 0}$	-		-13.10	-

[a] Neck & Kim (2001), [b] OECD (2001)

The data available for the equilibrium constants for the carbonate complexes are presented in Table 3. Most of the data is based on a semi-empirical model calculation (Neck & Kim (2000)). The stability constants of carbonato and hydroxo carbonato species are also given in Table 3. The uranyl (U(VI)) species are mainly carbonate species while U(IV) species remain hydroxo

214 species. Figure 1b presents the uranium pH – *E* diagrams for $2x10^{-2}$ M of CO_3 total. Analytical
215 domains are calculated using the data from Table 1, 2 and 3, and an Excel spreadsheet software.
216 The pH-*E* diagram calculated for a uranium concentration of 1 nM. In Figure 1b the
217 predominance pH-*E* diagram reveals that for a carbonate concentration of $2x10^{-2}$ M, in the
218 water stability region, the stable oxidation states are U(VI), U(V) and U(IV). The carbonato
219 complexes are namely the mono-, di- and tri- hydroxo complexes for U(VI) and the hydroxo
220 complexes are the mono-, di-, tri- and tetra-hydroxo complexes for U(IV). The U(V) does not
221 form complexes in the pH domain (2-6) for which it is observed

222
223 **Table 3.** Stability constants for the formation and hydrolysis species of uranium carbonates.
224 Data selected for $(UO_2)^{+2}(OH)_i(CO_3)_j^{(2-i-2j)+}$, $[UO_2]^{+}(OH)_i(CO_3)_j^{(1-i-2j)+}$, $U^{4+}(OH)_i(CO_3)_j^{(4-i-2j)+}$,
225 $U^{3+}(OH)_i(CO_3)_j^{(3-i-2j)+}$.
226

$\log K_{ij}$	U(VI)	U(V)	U(IV)	U(III)
$\log K_{01}$	9.94 [c]	5.120 [c]	13.7 [b]	6.5 [a]
$\log K_{11}$	-	-	-	-5.8 [a]
$\log K_{21}$	-	-	-	-7.9 [a]
$\log K_{02}$	6.67 [c]	1.8 [c]	10.6 [b]	5.3 [a]
$\log K_{12}$	-	-	-	-13.3 [a]
$\log K_{03}$	5.23 [c]	-1.895 [c]	7.6 [b]	1.6 [a]
$\log K_{04}$	-	-	3.3 [b]	-3.4 [a]
$\log K_{50}$	-	-	-1.2 [b]	-

227
228 [a] Data for Am, Hummel et al., (2002); [b] Data from Neck *et al*., (2000); [c] OECD (2003).
229

230

231

232

233

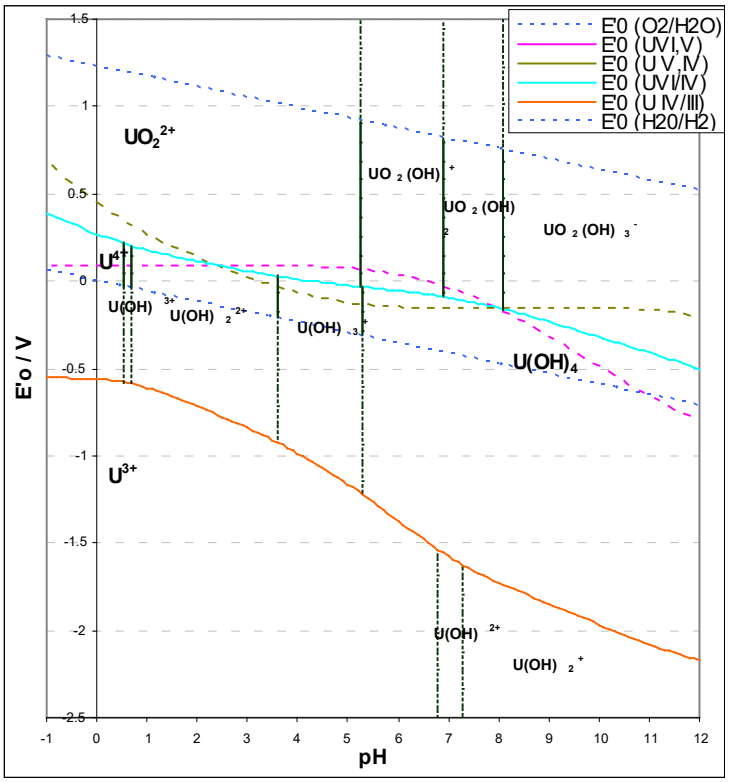

a

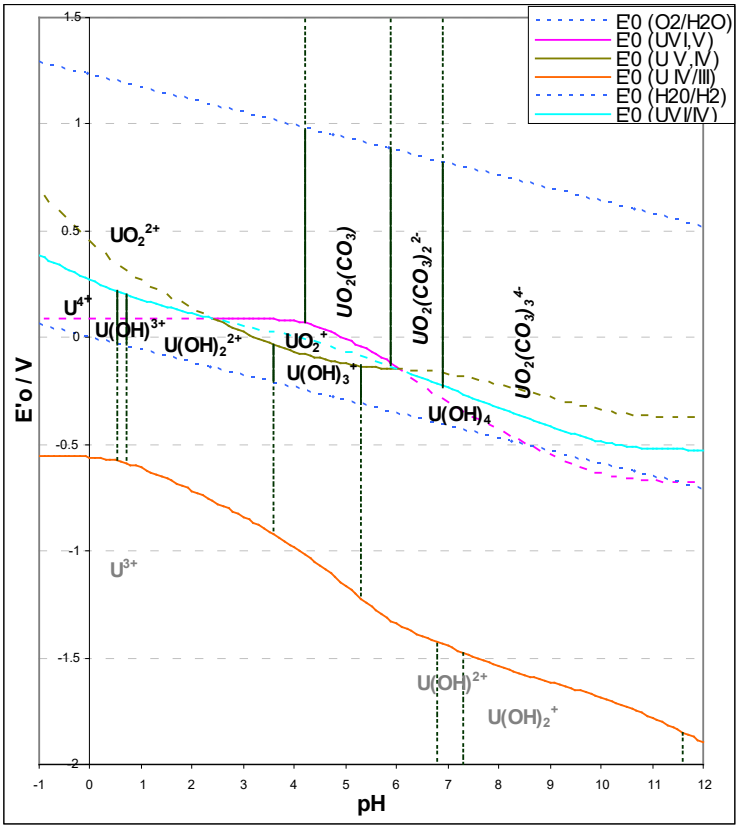

b

Fig. 1: Indicative uranium redox – pH plots for
a carbonate free and
b $2x10^{-2}$ M carbonate water

3.2 Simulation results for uranium sorption onto model particles

The uranium sorption onto Al_2O_3, FeOOH and SiO_2 has been simulated using Eq. 7.

The equilibrium constants $\log K_{i0}$ for the hydrolysed species ($[M^{+z}O_x](OH)_i^{(z-2x-i)+}$) for the U(III), (Degueldre *et al*. (1994), U(IV) (Hummel (2002)),U(V) (Neck *et al*., (2001)) and U(VI) (Thoenen (2000)) presented in Table 2 are systematically used for the calculations.

In Table 4 the correlation used for the calculation of the distribution coefficient of U using Eq. 7 for the three selected particulate materials: Al_2O_3, FeOOH and SiO_2, covered with >Al-OH, >Fe-OH and >SiOH sites, are given to apply the methodology suggested earlier Degueldre (1995) and Degueldre (1997). The applied correlations between the surface complexation constants $K_{s,i\text{-}1,0}$ and the hydrolysis constants $K_{i,0}$ are the link between hydrolysis and surface complexation. The $\log K_{s,i\text{-}1,0}$ - $\log K_{i,0}$ correlations given in Table 4 clearly show that the sorption on Al_2O_3, is stronger than on FeOOH and itself stronger than on SiO_2.

For the sorption, a site density of 3 nm^{-2} e.g. James & Parks (1982); Villalobos *et al* (2004), a particle size of 200 nm (specific surface ~ 10 $m^2\ g^{-1}$), a particle concentration of $1.7x10^{-3}$ g l^{-1} and density of 2 g cm^{-3} (arbitrary value) were used for the calculations. Distribution coefficients can be calculated (Eq. 8) using other parametric values. The computations were also performed using Excel spreadsheet software.

Table 4: Literature data used for the correlations between the surface complexation constants ($K_{s,i\text{-}1,0}$) and the hydroxo complex stability constants ($K_{i,0}$) and surface site (>AlOH, >FeOH and >SiOH) (de)protonation of the selected particles (Al_2O_3, FeOOH and SiO_2). Data from Hachyia *et al* (1984) for Al_2O_3, from Balistieri *et al* (1981) for FeOOH and from Righetto et al (1991) for SiO_2. .

	Al_2O_3	FeOOH	SiO_2
$\log K_{s,i-1,0}$	6.02 + 0.98 log $K_{i,0}$	3.75 + 0.75 log $K_{i,0}$	2.00 + 0.65 log $K_{i,0}$
pK_{a1}	5	4	-
pK_{a2}	10	10	7

The calculated distribution coefficients for uranium onto **Al_2O_3** particles (without or with carbonates) at different pH values are presented respectively in Figs. 2, where the solid lines indicate values inside the water stability region, while the dotted ones are outside of this area. Data reported at pH 2 and 12 are indicative; they are limited by eventual leaching that amplify in more acidic or basic media respectively as discussed in Section 2.2. Basically the domain of model validity should be between pH values from pK_{a1} to pK_{a2} when the >SuOH group predominate (see Table 4).

At pH 2 in a carbonate free system the redox effect of the U(III)/U(IV) couple is only visible (see Fig. 2a) around -0.75 V; whilst sorption increasingly above due to U(IV). A decrease is observed around +0.2 V due to U(VI) formation and its weaker sorption ability. At pH 4 the U sorption has increased and the U(IV) sorption takes place in reducing conditions (below E = 0 V). Hexavalent uranium U(VI) sorbs (weakly) in oxidising conditions. At pH 6 the sorption of both U(IV) and U(VI) are strong with log *Kd* around 5. At pH 8 and 10 the situation is similar. While at pH 12 sorption has decreased due to uranium speciation $U(OH)_5^-$ and $UO_2(OH)_3^-$ which species does not sorb for stoechiometric reasons.

In carbonated system (see Fig 2b), the log *Kd* vs *E* plots are marked by the absence of U(IV) carbonato complexes and the strong formation of U(VI) carbonato-complexes. In reducing conditions U(IV) sorption reaches log *Kd* values of 5 for pH 6 to 10 and decreases for pH 12 in the same fashion as for dicarbonated systems.

291 Fig 2
292
293

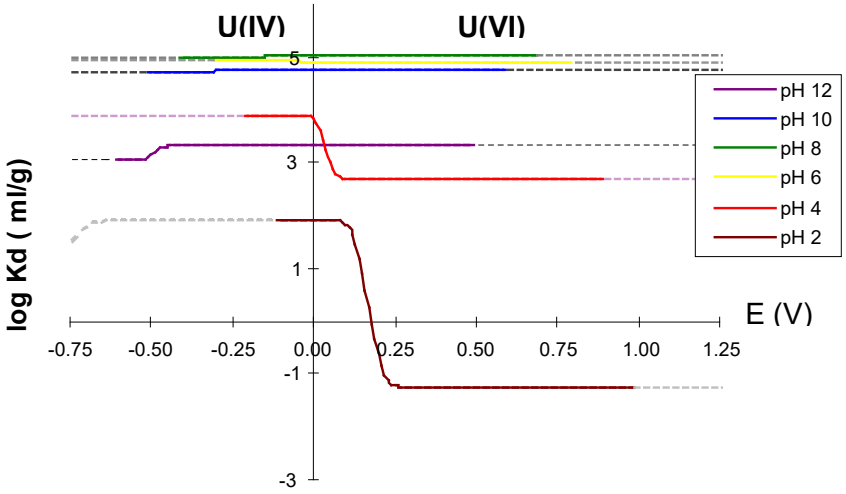

294 **a**
295

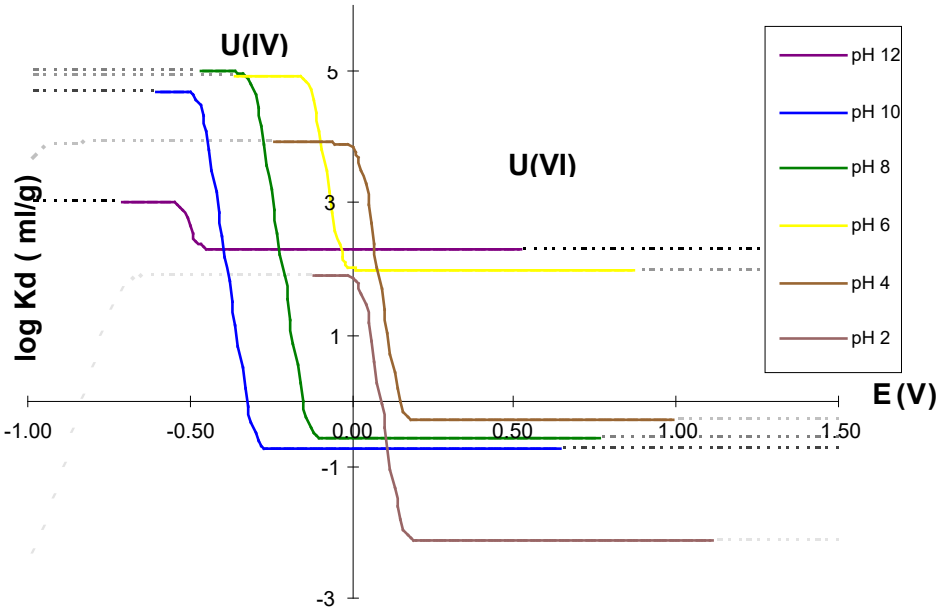

296 **b**
297
298 **Fig 2:** Uranium sorption on Al_2O_3: log *Kd* as a function of *E* and pH.
299 **a** carbonate free and
300 **b** $2x10^{-2}$ M carbonate water (indicative data for pH<6)
301
302

303 The sorption of U onto **FeOOH** particles can be seen in Fig. 3, the nature of sorbed species is
304 suggested by the redox diagram presented in Fig 1.
305 At pH 2 in carbonate free system the redox effect of the U(III)/U(IV) couple is only visible (see
306 Fig 3a) around -0.75 V, sorption increases with the *E* due to U(IV). A decrease is observed
307 around +0.2 V due to the increasing presence of U(VI). At pH 4 the U sorption has increased
308 with the U(IV) sorption taking place in reducing conditions while U(VI) undergoes (weaker)
309 sorption in oxidising conditions. At pH 6 the sorption of both U(IV) and U(VI) are strong with
310 log *Kd* around 4.0 to 4.5. At pH 8 and 10 the situation is similar, differentiated only by a slight
311 decrease under reducing conditions. At pH 12 sorption has decreased due to the U speciation
312 ($U(OH)_5^-$ and $UO_2(OH)_4^{2-}$ which do not sorb.
313
314 In carbonate system (Fig 3b), the log *Kd* vs *E* plots are marked by the absence of carbonato
315 complexes of U(IV) and the strong formation of U(VI) carbonato complexes. The log *K*d vs *E*
316 plots are marked by the absence of U(IV) carbonato complexes and the strong formation of
317 U(VI) carbonato complexes. In reducing conditions U(IV) sorption reach log *Kd* values of 5 for
318 pH 6 to 10 and decreases for pH 12 is observed for the reason reported above (limit of
319 validation of our methodology).
320

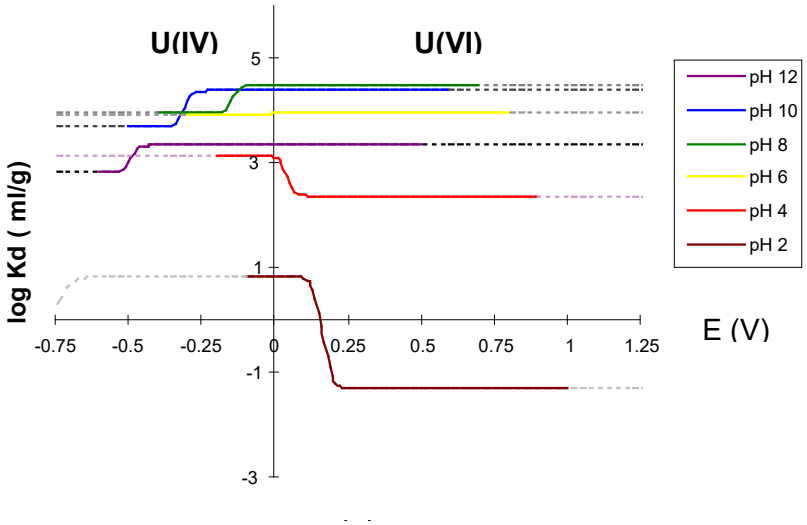

a

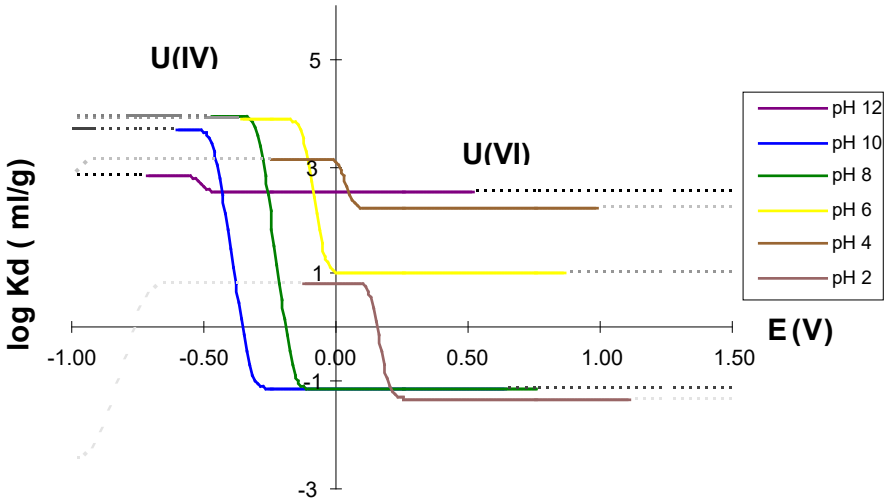

b

Fig 3: Uranium sorption on FeOOH: log *Kd* as a function of *E* and pH.
a carbonate free and
b $2x10^{-2}$ M carbonate water (indicative data for pH<6)

The uranium sorption behaviour onto **SiO_2** particles is depicted in Fig. 4. The sorbing species distribution can be guided by the redox diagram presented in Fig 1.

At pH 2 in carbonate free system the redox effect of the U(III)/U(IV) couple is also found (Fig 4a) around -0.75 V, the increase of sorption with *E* is due to the presence of U(IV). A decrease is observed around +0.2 V due to U(VI). At pH 4 the U sorption has increased and the U(IV) sorption takes place in reducing conditions while U(VI) sorbs (weaker) in oxidising conditions. At pH 6 the sorption of both U(IV) and U(VI) are strong with log *Kd* around 2.0 to 3.0. At pH 8 and 10 the situation is similar, a slight decrease is observed in reducing conditions. At pH 12 sorption has decreased due to the U speciation $U(OH)_5^-$ and $UO_2(OH)_4^{2-}$ which do not sorb.

In carbonate system (Fig 4b), the log *Kd* vs *E* plots are marked by the absence of carbonato complexes of U(IV) and the strong formation of U(VI) carbonato complexes. In reducing conditions U(IV) sorption reach log *Kd* values of 5 for pH 6 to 10 and decreases for pH 12 for the reason reported above.

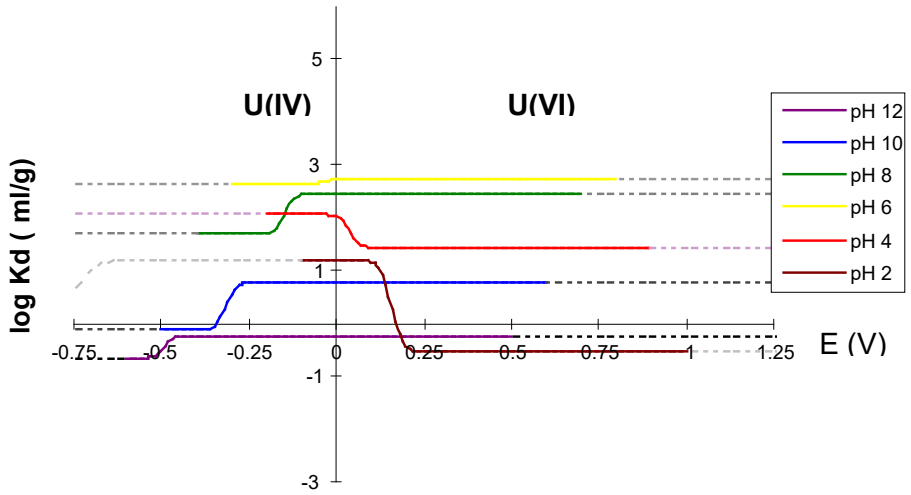

a

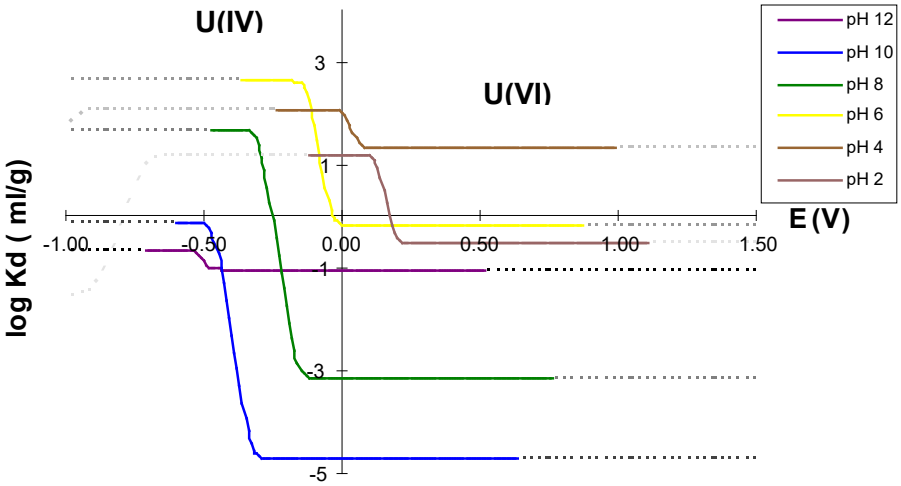

b

Fig 4: Uranium sorption on SiO_2: log *Kd* as a function of *E* and pH.
a carbonate free and
b $2x10^{-2}$ M carbonate water (indicative data for pH<6)

4. Discussion

The main species that drive the sorption on materials are those found in water and those at the surface of the sorbing phase. As displayed in the pH-*E* diagram of U, these are mainly the U(IV) and U(VI) species that are found in the stability domain of water. The U(III) species may be observed outside the stability domain of water while U(V) may be found marginally, as its concentration in its possible stability domain is low. In practice, the most useful redox parameter is the standard apparent redox potential *E*'°, which is defined as the potential at which in water 50% of the soluble forms are U(VI) and 50% U(IV), or, for the solid 50% of the sorption sites are occupied by U(VI) and 50% by U(IV). These issues had to be examined prior any discussion of the sorption results keeping in mind that the quality of the modelled speciation results is closely linked to the thermodynamic data as discussed by Mühr-Ebert *el al.* (2019).

4.1 Speciation in TIC free solution and their effect on sorption

The uranium speciation in aqueous solution plays a relevant role. Under normal saline (e.g. NaCl waters) conditions, it complexes from UO_2^{2+} to $[UO_2(OH)_i]^{2-I}$ according to it pH. Therefore the pH is an important parameter for the species in solution (see Fig.1) and after sorption at the surface of the particles. The log *Kd* increases from acidic to neutral solution for the 3 model materials and the 200 nm size show that the maximum sorption is observed in the pH domain 6 to 8 (see Table 5). The maximum log *Kd* increases from SiO_2 2.7 (pH 6, *E*>0 V) to 5.0 (pH 6 - 8, *E* [-0.5 - +0.7] V) for Al_2O_3 as could be anticipated from the data displayed in Table 4.

In contrast, the standard apparent redox potential *E*'° in solution is less oxidising at pH 2 than on the substrates because U(IV) sorbes (log *Kd*>0) while U(VI) does not (log *Kd* < 0). At pH 6, all E'° values are comparable, and for higher pH the E'° values on substrates become slightly more negative than that of the solution due to increasing activity of U(VI) compared to U(IV).

Table 5: Standard apparent redox potential E'° (V vs SHE) of the U(VI)/U(IV) couple in carbonate free solution and on the studied substrates as well as the log *Kd* (*Kd's* in mL g^{-1}) values for U(VI) and U(IV) on these substrates for given pH.

.pH	2	4	6	8	10	12
***E*'°/Solution**	+0.115	+0.026	-0.039	-0.128	-0.295	-0.474
log*Kd* U(VI)	-0.54	+1.44	+2.73	+2.47	+0.78	-0.23
***E*'°/SiO_2**	+0.160	+0.041	-0.028	-0.150	-0.318	-0.505
log*Kd* U(IV)	+1.20	+2,06	+2.63	+1.69	-0.12	-0.66
log*Kd* U(VI)	-1.32	+2.36	+3.94	+4.49	+4.37	+3.33
***E*'°/FeOOH**	+0.163	+0.051	-0.051	-0.143	-0.296	-0.490
log*Kd* U(IV)	+0.83	+3.14	+3.90	+3.94	+3.68	+2.82
log*Kd* U(VI)	-1.25	+2.68	+4.90	+5.04	+4.76	+3.32
***E*'°/Al_2O_3**	+0.177	+0.042	-0.052	-0.156	-0.313	-0.490
log*Kd* U(IV)	+1.91	+3.91	+4.95	+4.99	+4.70	+3.04

4.2 Speciation in TIC solution and their effect on sorption

As for the TIC-free aqueous solution, the uranium speciation in solution plays a central role. It goes from UO_2^{2+} to $UO_2(OH)_i]^{2-i}$ under saline (NaCl) water conditions or $[UO_2(CO_3)_3]^{4-}$ in solution with $NaHCO_3$, potentially $[Ca(UO_2)(CO_3)_3]^{2-}$ and $[Ca_2(UO_2)(CO_3)_3]$ in a $Na(Ca)HCO_3$ water as reported by Moulin *et al.* (1990). This was confirmed for artificial seawater by Beccia et al (2017).

The largest log *Kd* values for the 3 model materials and the 200 nm size show that the maximum sorption is observed in the pH domain 4 to 6 (see Table 6). The maximum log *Kd* increases from SiO_2 2.6 (pH 6, *E*<0V) to 5.0 (pH 6, *E*<0.1V) for Al_2O_3. Note that for pH < 6 TIC becomes very small and data are sketched, given in grey, for information.

The standard apparent redox potential *E*'° in solution is less oxidising at pH 2 than on the substrates because U(IV) sorbes (log *Kd*>0) while U(VI) does not (log *Kd* < 0). Below pH 6, TIC is very low. At pH 6, *E*'° values on substrates are slightly more positive than that of the solution due to larger activity of U(VI) compared to U(IV), and for higher pH the *E*'° values on substrates remain slightly more positive up to pH 12.

Table 6: Standard apparent redox potential *E'°* (V vs) of the U(VI)/U(IV) couple in $2x10^{-2}$ M carbonated solution and on the studied substrates as well as the log *Kd* (*Kd's* in mL g^{-1}) values for U(VI) and U(IV) on these substrates for given pH. Data for pH < 6 are sketched.

pH	2	4	**6**	**8**	**10**	**12**
***E*'°/Solution**	+0.117	+0.011	-0.128	-0.309	-0.468	-0.521
log*Kd* U(VI)	-0.54	+1.31	-0.19	-3.16	-4.72	-1.04
***E*'°/SiO_2**	+0.163	+0.042	-0.081	-0.233	-0.419	-0.500
log*Kd* U(IV)	+1.20	+2.06	+2.62	+1.68	-0.12	-0.66
log*Kd* U(VI)	-1.32	+2.23	+1.02	-1.14	-1.12	+2.52
***E*'°/FeOOH**	+0.166	+0.041	-0.097	-0.235	-0.401	-0.525
log*Kd* U(IV)	+0.83	+3.14	+3.89	+3.94	+3.68	+2.82
log*Kd* U(VI)	-2.13	-0.31	+1.98	-0.59	-0.74	+2.28
***E*'°/Al_2O_3**	0.185	0.080	-0.080	-0.225	-0.375	-0.500
log*Kd* U(IV)	+1.91	+3.91	+4.94	+4.99	+4.70	+3.01

4.3 Comparison of simulated and experimental sorption data

In environmental science, sorption has been treated originally as empirical, with data derived from batch tests and data listed for specific solid and liquid materials e.g. Puls *et al.* (1989).

Despite already existing body of works such as (Degueldre *et al*. 1994) applying actinide surface complexation for calculation of distribution coefficients, uranium sorption studies have been reviewed to assess the surface area normalisation for interpreting distribution coefficients, e.g. Payne *et al*. (2011) and completed by suggesting guidelines for thermodynamic sorption modelling in the context of radioactive waste disposal (Payne *et al*. (2013)). There have been some attempts to apply surface complexation for describing the sorption of Am(III) on model Al_2O_3 and SiO_2 as well as on clay particles, **Ref** Alonso & Degueldre (2003). Usually, Am(III) may be considered as an analogue of U(VI) and Th(IV) of U(IV).

The comparison of the uranium sorption properties on the studied model particles (e.g. 200 nm) of sorbent Fig's 2, 3 and 4 reveals that the uranium sorption onto Al_2O_3 particles is stronger (with a maximum of log *Kd* = ~5) than onto FeOOH (with a maximum of log *Kd* = ~4) or onto SiO_2 particles (with a maximum of log *Kd* = ~3), because different semi-empirical correlations for relating the surface complex constants with the hydrolysed ones (Table 4) were applied driven by decreasing intercept terms (for log *Ks* = 0). This is presumed to be due to the decrease of electronegativity of the matrix surface structural elements within >Su. Each of the semi-empirical correlations (Table 4), used to evaluate a specific distribution coefficient, relates the surface constants (unknown) with the hydrolysed ones (known). The comparison of experimental sorption data (from the cited literature) with the modelled data using Eq. 8 for the specific case is reported in Table 7.

The uranium sorption was found to be strong on **alumina** particles. The sorption behavior of uranium was justified by Froideval *et al*. (2006) on the basis of TRLFS and XAFS spectroscopy data identifying strong surface complexes. This sorption can be amplified by the synergism effect of phosphate as reported by Guo *et al.* (2009) and Galindo *et al*. (2010). Guo found U(VI) *Kd* of 80 mL g^{-1} (log *Kd* ~2) for a particle specific surface of 130 m^2 g^{-1} (corresponding

to ~50 nm particles) at pH 4.4. This pH is however below the identified log *Kd* plateau of U(VI) on alumina but the log *Kd* value is comparable with its modelled value (Eq. 7). The americium sorption was found to be strong on alumina with log *Kd* = 3 for particle sizes ~50 μm and pH 7- 8 by Moulin *et al*. (1992). The Am(III) log *Kd* is around 3 between pH 6 and 8 for specific surface of 0.07 m^2 g^{-1}.

The binary and ternary surface complexes (hydroxo- carbonato) of U(VI) on the gibbsite/water interface were subsequently studied by Gückel *et al.* (2012) using vibrational and EXAFS spectroscopy. The U concentration is rather high and uranium dimers complexes are observed. This work was completed by Müller *et al*. (2013) investigating by in situ spectroscopy the surface reactions of U(VI) on γ-Al_2O_3 up to the transition from surface complexation to surface precipitation as studied for Th(IV) by Degueldre & Kline (2007) for Th(IV). These reactions (dimer- polymer- formation and surface precipitation) enhance the *Kd* values.

The reversibility of uranium and thorium binding on a modified bauxite refinery residue was investigated Clark *et al*. (2015). These authors found *Kd* values of 3000 mL g^{-1} in the pH above 4 and below 7. Finally, Mei *et al*. (2015) reported about the effect of silicate on U(VI) sorption to γ-Al_2O_3. However this batch study focusing mainly on U EXAFS, the U(VI) concentration is quite high ($6x10^{-5}$ M) for 1 g l^{-1} γ-Al_2O_3 colloids (*d* ~20 nm) which saturates the sites and which reduces apparently sorption (excess soluble) with an apparent log *Kd* = 3.3 .

The approach followed for Al_2O_3 model particles may be applied for the sorption of U onto montmorillonite and illite particles that have strongly reactive aluminol groups (>AlOH) on the edges (Degueldre *et al*, 1994). On montmorillonite, Bradbury & Baeyens (2005) found log *Kd* = 5.3 at pH 7 for particle sizes <500 nm (e.g. 200 nm) which also is comparable with our modelling result see Table 7. To complete the picture, Marques Fernandes, *et al* (2012) studied the sorption of U(VI) on montmorillonite in the absence and presence of carbonate and observed that the sorbed U(VI) fraction decreases with the carbonate concentration.

475

476 Uranium has also been investigated on **iron oxo-hydroxide** substrates. Murphy *et al*. (1999)
477 reported about the sorption of thorium (IV) and uranium (VI) to hematite in the presence of
478 natural organic matter. On 9 g l^{-1} 66 nm Fe_2O_3 they found 50% sorption at pH 4 or a log *Kd* of
479 about 2.0 while modelling (with Eq. 7) predicts log *Kd* = 1.5; the equilibrium is however not
480 reached in these tests. Similarly, Missana *et al*. (2003) investigated experimentally and by
481 modeling the U(VI) sorption on goethite. They found log *Kd* of 5.2 for goethite needles of
482 50x50x5000 nm (*d* ~1000 nm) at pH >5. Similar work was also performed by the same group
483 (Missana *et al*. (2003)) with **U(VI)** sorption on **magnetite** particles under anoxic environment.
484 For batch data (pH 4, 100 nm colloids, *M*/*V*= 2 g l^{-1}, [U(VI)]= 4x10^{-7} M) Values of log *Kd* (3.3)
485 are calculated from the batch data (pH 4, 100 nm colloids) and compared to the modelled one
486 (3.2) for 200 nm particles, for sorbed U(VI) the log *Kd* would be 2.5. This indicates that
487 reduction can take place during surface complexation. Wang *et al*. (2015) investigated the
488 sorption of **U(IV)** on magnetite. Values of log *Kd* (3.3) are calculated from the batch data (pH
489 4, 100 nm colloids, *M*/*V*= 2 g l^{-1}, [U(IV)]= 10^{-8} M) and compared to the modelled one (3.2) for
490 200 nm particles.

491 Uranium partitioning tests were also performed on ferrihydrite by Hiemstra *et al*. (2009), by
492 Foerstendorf *et al*. (2012) and more recently by Dublet *et al.* (2017). Dalvi *et al*. (2014) found
493 that the Th(IV) / U(VI) *K*d ratio was of the order of 17 (±5) between pH 7.78 and 8.42 for
494 sediment samples. This is very difficult to compare the results gained with the proposed model
495 at pH 8 (see Fig. 2,3,4) because the calculation results are very sensitive with carbonate
496 concentration and this data is not fixed in Dalvi *et al* (2014).

497

498 Finally, sorption work of uranium was also carried on **SiO_2.** Dent *et al*. (1992) reported on a
499 EXAFS study of uranyl ion in solution and sorbed onto **silica** and montmorillonite clay

colloids. On 80 nm silica colloids, at pH 4 the experimental log *Kd* was found to be 2.5 and the modelled data using Eq.8 gives a log *Kd* of 2.8 for the data describe earlier and for pH 4. Table 7 presents other results from Dent et al (1992)[55] and the modelled log *Kd* data for comparison.

Since Th(IV) can be considered as an analogue of U(IV) one can also report the work of Östhols (1995) on thorium sorption on amorphous silica to support the data. Quartz that is less sorbing that silica was investigated by Froideval *et al*. (2003). The U(VI) sorption on silica was also more recently tested for its effect by complexing anions by Kar *et al*. (2012). On silica like on other substrate materials, phosphorous derived groups may act as specific ligand such as silica-tethered phosphonic acid sorbents for uranium species from aqueous solution as investigated by Dudarko *et al*. (2015).

Finally, Stamberg, *et al* (2003), also studied uranyl ion sorption on silica of mesoporous nature. They also applied surface complexation modeling to investigate the processes occurring in the batchs focusing on the effect of carbonate. Without carbonate at pH 7.5, 98.6% uranium sorbed, while with 0.015 M carbonate the sorption droped to 88.2% on the porous silica.

Table 7: Comparison of the log Kd_e (±0.5) experimental and log Kd_m (*Kd's* in mL g^{-1}) modelled for the studied sorbing materials (size, particle; density 2 g cm^{-3}, site density 3 nm^{-2}, * clay) and solution of given pH, TIC.

Substrate M (g l^{-1})	An(X)	pH	TIC (M)	Size (nm)	log Kd_e	Log Kd_m	Conditions Size (nm)	References
Al_2O_3	U(VI)	4.4	-	50	2.0	2.8	.pH 4	Guo et al (2009)
Al_2O_3	Am(III)	6-8	-	50,000	3.0	3.2	20,000 pH 6	Moulin et al (1992)
Al_2O_3	U(VI)	6	-	(20,000)	3.3	3.0	20,000 pH 6	Clark et al (2015)
>AlOH*	U(VI)	7	-	(200)	3.3	3.0	200 pH7	Bradbury et al (2005)
>AlOH*	U(VI)	6	-	(200)	3.3	3.0	200 pH 8	Marques et al (2012)
>AlOH*	U(VI)	8	$5x10^{-3}$	(200)	1.5	0.0	200 pH 8	Marques et al (2012)
FeOOH	U(VI)	>5	-	1000	5.2	4.5	200	Missana et al (2005)
Fe_3O_4	U(VI)	4	-	100nm	3.3	3.2	200	Missana et al (2005)
Fe_3O_4	U(IV)	4	-	100nm	3.3	3.2	200	Wang et al (2011)
SiO_2	Am(III)	6-8	-	50,000	2.5	2.8	200	Moulin et al (1992)
5000 SiO_2	U(VI)	4	-	80	2.5	2.8	200	Dent et al (1992)
5000 SiO_2	U(VI)	6	-	80	4	2.9	200	Dent et al (1992)
500 SiO_2	U(VI)	4	-	30	3.1	2.4	20	Dent et al (1992)
5000 SiO_2	U(VI)	4	-	30	2.8	2.4	20	Dent et al (1992)

In the case of **composite** minerals, the above studied methodology can be applied. This is confirmed in Manoj *et al.* (2020) work, log *Kd* increases up to pH 6 after a plateau it gradually decreases for higher pH (see data in Tables 5 and 6). Their log *Kd* values are lower than us because their particle sizes are larger than our model particles. One important body of work to note concerning redox reactions of uranium at the surface of inorganic sorbents is the work of Descorte *et al*. (2010). It concerns direct reduction in the context of **pyrite** interaction with U(VI). In this case data show a maximal cation uptake above pH 5.5. Concentration isotherms

for U(VI) sorption on pyrite indicate specific behaviours. In the U(VI) case, sorption seems to occur on two different sites with a total saturation concentration of 4.5×10^{-8} mol g^{-1}. At lower concentration, uranyl reduction occurs in U(IV), limiting the concentration of dissolved uranium to the solubility of UO_2(s) and the formation of a hyperstoichiometric UO_{2+x}(s). The results are consistent with a chemistry of the pyrite surface governed by S groups which can either sorb cations and protons, or sorb and reduce redox-sensitive elements such as U(VI).

To complete this study it must be mentioned that the model presented is unfortunately not designed to deal with uranium sorption on calcite. This is due to co-precipitation and formation of specific Ca-UO_2-CO_3 phases that are identified by advanced spectroscopic techniques such as EXAFS e.g. Reeder *et al*. (2004), Elzinga *et al* (2004). However, Butchins *et al*. (2006) found that uranium has a high affinity for calcite over a wide range of initial uranium concentrations (10^{-12} to 10^{-3} M) with $20 < Kd < 90$ (ml g^{-1}). The authors however do not specify the pH and the particle size of the material. In addition, Sturchio *et al* (1998) reported on tetravalent uranium in calcite using XAFS and micro-XAS.

Field studies were conducted by Curtis *et al* (2004) in an alluvial aquifer at a former U mill tailings site, by suspending approximately 10 g samples for periods of 3 to 15 months. Adsorbed U(VI) on these samples was determined by extraction. In situ K_d values calculated from the measurements of adsorbed and dissolved U(VI) ranged from **0.50 to 10.6 mL g^{-1}** and the K_d values decreased with increasing groundwater alkalinity. Curtis *et al* (2004) found a good agreement between the predicted *K*d's from surface complexation modeling and from measured in situ K_d values.

Experimental and modelled log *Kd* data are comparable. However, the quality of data is affected by their precision and accuracy. The main factors that are relevant for data calculation are the site density which may vary from 1 to 10 nm^{-2}, the state of the surface since the bulk composition (density) may be different from the surface (contaminations by other active groups than the expected one) and the uncertainty in the reported particle size. Actually, particles are

554 seldom mono-dispersed but poly-dispersed and their size distributions are not always accurately
555 surface weighted. Particle specific surfaces are currently determined by gas sorption however
556 these derived data are not provided by ionic sorption.
557 The model applied considers also the correlation between the stepwise hydrolysis constants and
558 the stepwise surface complexation constants. It is consequently impossible to calculate the
559 surface complexation constant for the last hydrolysed species. The lack of surface constants in
560 the calculations limits the applicability of the model in the high pH range where the last
561 hydrolysed species is predominant (justifying our pH upper limit to 12), but in spite of this
562 limitation the model gives satisfactory results in a wide range of conditions.
563 Uranium contamination of soil has been a major concern with respect to its toxicity and
564 persistence in the environment, Selvakumar *et al* (2018). Owing to these problems, remediation
565 of uranium-contaminated soils has been investigated by various techniques and the authors
566 hope that this study can help to remediate contaminated sites.
567
568 **5. Conclusions**
569
570 A model that relates the distribution coefficient with the redox potential was developed for
571 evaluating the effect of the redox potential on the sorption of uranium onto model substrates.
572 The model includes surface complexation and complexation with ligands. It also considers the
573 effect of the redox potential for all the species at the surface and in solution. The model was
574 applied to uranium, as an important safety relevant redox sensitive element, and the calculated
575 distribution coefficient values confirmed that the redox potential does affect the sorption of U
576 in the site stability domain and in the water stability region and outside. The calculated values
577 are in relative agreement with scare experimental values reported in the literature. This model is
578 applicable to other redox sensitive elements.

The sorption analysis so far provides good predictive values for a limited subset of the experimental data, allowing approximate predictive modelling of the partition coefficients for a variety of groundwaters. Such data may help to understand the formation of ore deposits (U(VI) => U(IV)) or contribute to search a versatile U extraction protocol from seawater. Effect of organics shall be discussed in a future study. This last target would require to expanding the variety of absorption substrate being considered.

Finally, work is to be undertaken to represent oxidation/reduction systems within the modelling, to represent reductive deposition on the surfaces to complete U sorption by UO_2 precipitation onto the substrate.

Appendices

Six "logKd Vs E" EXCEL spreadsheets are included: 3 for carbonate free solutions and 3 for carbonate solution. They concern Kd calculations for the sorption of U on Al_2O_3, FeOOH and SiO_2. Each spreadsheet includes sub-sheets for pH: 0, 2, 4, 6, 8, 10 and 12, as well as one resume. Each pH sub-sheet presents the detailed data calculations. The resumes sub-sheet present the "logKd Vs E" graphs for pH 2 to 12 for the substrates and for the carbonated solution conditions.

References

Alonso & Degueldre, (2003)
Alonso U., Degueldre C.,
Modelling americium sorption onto colloids: effect of redox potential.
Coll. Surf. A, 217 (2003) 55-62. doi:10.1016/S0927-7757(02)00558-7

Baeyens et al (2005)
Baeyens B., Bradbury M.,. **Modelling the sorption of Mn(II), Co(II), Ni(II), Zn(II), Cd(II), Eu(III), Am(III), Sn(IV), Th(IV), Np(V) and *U(VI)* on montmorillonite: Linear free energy relationships and estimates of surface binding constants for some selected heavy metals and actinides**. Geochim. Cosmochim. Acta, 69 (2005) 262-277.
https://doi.org/10.1016/j.gca.2004.07.020

Balistrieri et al (1981)

Balistrieri L., Brewer P., Murray J., **Scavenging residence times of trace metals and surface chemistry of sinking particles in deep ocean**. Deep-Sea Res. 28 (1981) 101–121. https://doi.org/10.1016/0016-7037(87)90208-0

Beccia et al (2017),
Beccia M.R., Matara-Aho M., Reeves B., Roques J., Den Auwer C., **New insight into the ternary complexes of uranyl carbonate in seawater**. J. Environm. Radioactivity, 178–179 (2017) 343-348. https://doi.org/10.1016/j.envrad.2017.08.008

Butchins et al (2006),
Butchins L.J.C., Lievens F.R., Vaughan D.J., Wincott P., **Using surface imaging and analytical techniques to study the calcite surface in contact with UO_2^{2+} ions**. Proceed. Recent Advances in Actinide Sci., RSC, (2006) 65-66 .

Chisholm-Brause et al (2004),
Chisholm-Brause C. J., Berg J. M, Little K. M., Matzner R. A., Morris D. E., .
Uranyl sorption by smectites: spectroscopic assessment of thermodynamic modeling.
J. Coll. Interf. Sci., 277 (2004) 366-382. https://doi.org/10.1016/j.jcis.2004.04.047

Clark et al (2015),
Clark M.W., Payne T.E., Harrison J.J., Comarmond M.J., Reichelt-Brushett A.J.,. **Reversibility of uranium and thorium binding on a modified bauxite refinery residue: The effects of aging temperature**,
Appl. Geochem., 53 (2015) 79-90, https://doi.org/10.1016/j.apgeochem.2014.12.011

Curtis et al (2004)
Curtis G. P., Fox P., Kohler M., Davis J. A., **Comparison of in situ uranium KD values with a laboratory determined surface complexation model**, Appl. Geochem., 19 (2004) 1643-1653

Dalvi et al (2014)
Dalvi A.A., Kumar S.D., Reddy A. V. R., **A site-specific study on the measurement of sorption coefficients for radionuclides**, Int. J. Environ. Sci. Technol., 11 (2014) 617–622

Degueldre et al (1994),
Degueldre C., Ulrich H.J., Silby H.,
Sorption of 241-Am onto montmorillonite. illite and hematite colloids.
Radiochim. Acta 65 (1994) 173-179. https://doi.org/10.1524/ract.1993.62.12.81

Degueldre et al (1995).
Degueldre C., **Retention of Redox Sensitive Elements: the Case of Neptunium**,
J. Environ. Radioactivity, 29 (1995) 75-87. https://doi.org/10.1016/0265-931X(95)00021-2

Degueldre (1997),
Degueldre C., **Retention of Redox Sensitive Elements: The Case of Neptunium in Aquifers**.
J. Environ. Radioactivity, 34 (1997) 211-214.
https://doi.org/10.1016/0265-931X(96)00032-X

Degueldre et al (1999),

C. Degueldre, F. Rocchiccioli, A. Laube, **Accelerated measurement of groundwater redox potentials: method and application.** Anal. Chim. Acta, 396 (1999) 23-31. https://doi.org/0.1016/S0003-2670(99)00352-9

Degueldre & Kline (2007),
Degueldre C., Kline A., **Study of thorium association and surface precipitation on colloids.** Earth and Planet. Sci. Lett., 264 (2007) 104–113. https://doi.org/10.1016/j.epsl.2007.09.012

Degueldre & Bolek, (2009)
Degueldre C., Bolek M., **Modelling colloid association with plutonium: the effect of pH and redox potential.**
Appl. Geochem., 24, 310-318. https://doi.org/10.1016/j.apgeochem.2008.10.008

Degueldre et al. (2019),
Degueldre C.A., Dawson R.J., Najdanovic-Visaka V., **Nuclear fuel cycle, with a liquid ore and fuel: toward renewable energy**. Sustainable Energy & Fuels, 3 (2019) 1693-1700. https://doi.org/10.1039/C8SE00610E

Dent et al (1992),
Dent A. J, Ramsay J. D. F, Swanton S. W., **An EXAFS study of uranyl ion in solution and sorbed onto silica and montmorillonite clay colloids**. J. Coll. Interf. Sci., 150 (1992) 45-60. https://doi.org/10.1007/BF00877274

Descostes et al (2010)
Descostes M., Schlegel M. L., Eglizaud N., Descamps F., Simoni E.,. **Uptake of uranium and trace elements in pyrite (FeS_2) suspensions**, Geochim. Cosmochim. Acta, 74 (2010) 1551-1562. https://doi.org10.1016/J.GCA.2009.12.004

Dublet et al (2017)
Dublet G., Lezama Pacheco J., Bargar J. R., Fendorf S., Kumar N., Lowry G., Brown G. E., (2017). **Partitioning of uranyl between ferrihydrite and humic substances at acidic and circum-neutral pH**, Geochim. Cosmochim. Acta, 215 (2017) 122-140. https://doi.org/10.1016/j.gca.2017.07.013

Dudarko (2015)
Dudarko O. A., Gunathilake C., Wickramaratne N. P., Sliesarenko V. V., Jaroniec M.,. **Synthesis of mesoporous silica-tethered phosphonic acid sorbents for uranium species from aqueous solutions**, Coll. Surf. A, 482 (2015) 1-8. https://doi.org/10.1016/j.colsurfa.2015.04.016

Elzinga, et al (2004)
E. J. Elzinga, C. D. Tait, R. J. Reeder, K. D. Rector, Robert J.Donohoe, D. E. Morris, **Spectroscopic investigation of U(VI) sorption at the calcite-water interface,** Geochim. Cosmochim. Acta, 68 (2004) 2437-2448

Foerstendorf et al (2012)
Foerstendorf H., Heim K., Rossberg A., **The complexation of uranium(VI) and atmospherically derived CO_2 at the ferrihydrite–water interface probed by time-resolved vibrational spectroscopy,** J. Coll. and Interf. Sci., 377 (2012) 299-306. https://doi.org/10.1016/j.jcis.2012.03.020.

Froideval et al (2003),
Froideval A., Del Nero M., Barillon R., Hommet J., Mignot G., **pH dependence of uranyl retention in a quartz/solution system: an XPS study.** J. Coll. Interf. Sci., 266 (2003) 221-235. https://doi.org/10.1016/S0021-9797(03)00528-9

Froideval et al (2007),
Froideval A., Del Nero M., Gaillard C., Barillon R., Rossini I, Hazemann J. L., **Uranyl sorption species at low coverage on Al-hydroxide: TRLFS and XAFS studies**. Geochim. Cosmochim. Acta, 70 (2007) 5270-5284. https://doi.org/10.1016/j.gca.2006.08.027

Galindo et al (2010),
Galindo C., Del Nero M., Barillon R., Halter E., Made B.,. **Mechanisms of uranyl and phosphate (co)sorption: Complexation and precipitation at α-Al_2O_3 surfaces**, J. Coll. Interf. Sci., 347 (2010) 282-289 e https://doi.org/10.1016/j.jcis.2010.03.045

Gavrilescu et al (2008)
Gavrilescu M., Pavel L.V., Cretescu I.,.
Characterization and Remediation of Soils Contaminated with Uranium.
J. Hazardous Mater., 163 (2008) 475-510. https://doi.org/10.1016/j.jhazmat.2008.07.103

Grenthe et al (1992)
Grenthe I., Stumm W., Laaksoharju M., Nilsson A.-C., Wikberg P.,
Redox potentials and redox reactions in deep groundwater systems,
Chem. Geol., 98 (1992) 131-150.
https://doi.org/10.1016/0169-7722(95)00037-2

Gückel et al (2012)
Gückel K., Rossberg A., Brendler V., Foerstendorf H., **Binary and ternary surface complexes of U(VI) on the gibbsite/water interface studied by vibrational and EXAFS spectroscopy**, Chem. Geology, 326–327 (2012) 27-35.
https://doi.org/10.1016/j.chemgeo.2012.07.015

Guo et al. (2009)
Guo Z., Yan C., Ji. Xu, Wu W.,
Sorption of U(VI) and phosphate on γ-alumina: Binary and ternary sorption systems,
Coll. Surf. A:, 336 (2009)123-129. https://doi.org/10.1016/j.colsurfa.2008.11.032

Hachiya et al (1984)
Hachiya K., M. Sasaki M., Saruta Y., Mikami N., Yasumaga, T., **Static and kinetic studies of adsorption–desorption of metal ions on a γ-Al_2O_3 surface: 1. Static studies on adsorption–desorption.** J. Phys. Chem. 88 (1984) 23–27. https://doi.org/10.1021/j150645a007

Hiemstra et al (2009)
Hiemstra T., Van Riemsdijk W. H., Rossberg A., Ulrich K.-U., **A surface structural model for ferrihydrite II: Adsorption of uranyl and carbonate,** Geochim. Cosmochim. Acta, 73 (2009) 4437-4451. https://doi.org/10.1016/j.gca.2009.04.035

Hummel et al (2002)
Hummel W., Berner U., Curti E., Pearson F.J., Thoenen T.. **Nagra/PSI Chemical Thermodynamic Data Base 01/01**. Radiochim. Acta, 90 (2002) 805-813.

James & Parks (1982).
James R., Parks G., **Characterisation of aqueous colloids by their electrical double-layer and intrinsic surface chemical properties**. In Surface and Colloid Science, ed E. Matijevic, Plenum Press, London, (1982) pp. 119-217. https://doi.org/10.1007/978-1-4613-3204-6

Kar et al (2012).
Kar A. S., Kumar S., Tomar B. S., **U(VI) sorption by silica: Effect of complexing anions,** Coll. Surf. A, 395 (2012) 240-247. https://doi.org/10.1016/j.colsurfa.2011.12.038.

Katz et al (1986)
Katz J.J., Seaborg G.T., Morss L.R., **The chemistry of actinide elements V1.**
2nd Ed., Chapman & Hall, London, (1986). https://doi.org/10.1007/1-4020-3598-5

Lefèvre et al (2008).
Lefèvre G., Kneppers J., Fédoroff M.,
Sorption of uranyl ions on titanium oxide studied by ATR-IR spectroscopy,
J. Coll. Interf. Sci., 327 (2008) 15-20. https://doi.org/10.1016/j.jcis.2008.07.044

Li et al (2019).
Li P., Wang J., Wang Y., Liang J., Wang X.,
Photoconvertion of U(VI) by TiO_2: an efficient strategy for seawater uranium extraction,
Chem. Engin. J., 365 (2019) 231-241. https://doi.org/10.1016/j.cej.2019.02.013

Lomenech et al (2003).
Lomenech C., Simoni E., Drot R., Ehrhardt J. -J, Mielczarski J.,.
Sorption of uranium (VI) species on zircon: structural investigation of the solid/solution interface. J. Coll. Interf. Sci., 261 (2003) 221-232. https://doi.org/10.1063/1.47506

Manoj et al (2020).
Manoj S., Thirumurugan M., Elongo L., **Determination of distribution coefficient of uranium from physical and chemical properties of soil**. Chemosphere, 244 (2020) 125411.
https://doi.org/10.1016/j.chemosphere.2019.125411

Marques Fernandes et al (2012).
Marques Fernandes M., Baeyens B., Dähn R., Scheinost A.C., Bradbury M.H., **U(VI) sorption on montmorillonite in the absence and presence of carbonate: A macroscopic and microscopic study**, Geochim. Cosmochim. Acta, 93 (2012) 875-892.
https://doi.org/10.1016/j.gca.2012.04.017

Mei et al (2015).
Mei H., Tan X., Yu S., Ren X., Wang X., **Effect of silicate on U(VI) sorption to γ-Al_2O_3: Batch and EXAFS studies.** Chem. Engin. J., 269 (2015) 371-378.
https://doi.org/10.1016/j.cej.2015.01.121

Missana et al (2003a).
Missana T., García-Gutiérrez M., Maffiotte C., **Experimental and modeling study of the uranium (VI) sorption on goethite**, J. Coll. Interf. Sci., 260 (2003) 291-301. https://doi.org/10.1016/s0021-9797(02)00246-1

Missana et al (2003b).

Missana T., García-Gutiérrez M., Fernańdez V., **Uranium (VI) sorption on colloidal magnetite under anoxic environment: experimental study and surface complexation modelling**. Geochim. Cosmochim. Acta, 67 (2003) 2543-2550. https://doi.org/10.1016/S0016-7037(02)01350-9.

Moulin et al (1990)
Moulin C., Beaucaire C., Decambox P., Mauchien M., **Determination of uranium in solution at the ng 1^{-1} level by time-resolved laser-induced spectrofluorimetry: application to geological samples**. Anal. Chim. Acta, 238, 291-296. https://doi.org/ 10.1016/S0003-2670(00)80550-4

Moulin et al (1992)
Moulin V., Stammose D., Ouzounian G., **Actinide sorption at oxide-water interfaces: application to α alumina and amorphous silica.** Applied Geochemistry, 7 (1992) 163-166. https://doi.org/10.1016/S0883-2927(09)80072-3

Mühr-Ebert et al (2019).
Mühr-Ebert E.L., Wagner F., Walter C., **Speciation of uranium: Compilation of thermodynamic database and ist experimental evaluation using different analytical techniques**, Appl. Geochem., 100 (2019) 213-222

Müller et al (2013).
Müller K., Foerstendorf H., Brendler V., Rossberg A., Gröschel A., **The surface reactions of U(VI) on γ-Al_2O_3 — In situ spectroscopic evaluation of the transition from sorption complexation to surface precipitation**. Chem. Geology, 357 (2013) 75-84. https://doi.org/10.1039/c3dt50814e

Murphy et al (1999).
Murphy R. J., Lenhart J. J., Honeyman B. D., (1999). **The sorption of thorium (IV) and uranium (VI) to hematite in the presence of natural organic matter**. Coll. and Surf. A, 157 (1999), pp. 47-62. https://doi.org/10.1007/s10967-007-1120-2

Neck & Kim, (2000)
Neck V., Kim J.I.,. **An electrostatic approach for the prediction of actinide complexation constants with inorganic ligands**, Radiochim. Acta, 88 (2000) 815-822. https://doi.org/ 10.1524/ract.2000.88.9-11.815

Neck & Kim, (2001),
Neck V., Kim J.I., (2001). **Solubility and hydrolysis of tetravalent actinides**, Radiochim. Acta, 89 (2001) 1-16. https://doi.org/10.1524/ract.2001.89.1.001

OECD (2001),
OECD, **Chemical Thermodynamics of Uranium.** From OECD- Nuclear Energy Agency, Themodynamic data base project. (2001) https://doi.org/

OECD (2003),
OECD, **Chemical Thermodynamics**, Vol 5. From OECD- Nuclear Energy Agency, Themodynamic data base project. (2003) https://doi.org/

Östhols, (1995)

Östhols, E., **Thorium sorption on amorphous silica**. Geochim. Cosmochim. Acta, 59 (1995) 1235-1249. https://doi.org/10.1016/0016-7037(95)00040-7

Payne et al (2011),
Payne T. E., Brendler V., Comarmond M.J., Nebelung C., Steudtner R.,.
Assessment of surface area normalisation for interpreting distribution coefficients (Kd) for uranium sorption, J. Environm. Radioactivity, 102 (2011) 888-895. https://doi.org/ 10.1016/j.jenvrad.2010.04.005

Payne et al (2013),
Payne T. E., Brendler V., Ochs M., Baeyens B., Altmann S.,
Guidelines for thermodynamic sorption modelling in the context of radioactive waste disposal,
Environm. Modelling & Software, 42 (2013) 143-156.
https://doi.org/ 10.1016/j.envsoft.2013.01.002

Puls et al (1989).
Puls R. W., Ames L. L., McGarrah J. E., **The use of batch tests as a screening tool for radionuclide sorption characterization studies, Hanford, Washington, USA.** Applied Geochem., 4 (1989) 63-77. https://doi.org/10.1016/0883-2927(89)90059-0

Reeder et al (2004).
Reeder R.J., Nugent M., Tait C.D., Morris D.E., A. Lanzirotti A., **Spectroscopic investigation of U(VI) sorption at the calcite-water interface**, Geochim. Cosmochim. Acta, 68 (2004) 4799-4808

Richter et al (2016).
Richter C., Müller K., Drobot B., **Macroscopic and spectroscopic characterization of uranium(VI) sorption onto orthoclase and muscovite and the influence of competing Ca^{2+}**,
Geochim. Cosmochim. Acta, 189 (2016) 143-157. https://doi.org/ 10.1016/j.gca.2016.05.045

Righetto et al (1991)
Righetto L., Bidoglio G., Azimonti G., Bellobono, I., (1991). **Competitive actinide interaction in colloidal humic acid–mineral oxide systems.**
Environ. Sci. Technol. 25 (1991) 1913–1919. https://doi.org/10/1021/es00023a012

Selvakumar et al (2018)
Selvakumar R., Ramadoss G., Menon M.P., Rajendran K., Megharaj M.,
Challenges and complexities in remediation of uranium contaminated soils: A review,
J. Environmental Radioactivity, 192 (2018) 592-603.
https://doi.org/10.1016/j.jenvrad.2018.02.018

Silva et al (1995).
Silva R.J., Bidoglio G., Rand M.H., Robouch P.B., Wanner H., Puigdomenech I.,
Chemical Thermodynamics Vol. 2. **Chemical Thermodynamics of Americium**.
Ed. North Holland. Elsevier (1995). https://doi.org/ 10.1023/A:1023339723535

Singhal et al (2017).
Singhal P., Jha S. K., Pandey S. P., Neogy S.,
Rapid extraction of uranium from sea water using Fe_3O_4 and humic acid coated Fe_3O_4 nanoparticles,

J. Hazardous Mater., 335 (2017) 152-161. https://doi.org/10.1016/j.jhazmat.2017.04.043

Stamberg et al (2003).
Stamberg K., Venkatesan K.A., Vasudeva Rao P.R., **Surface complexation modeling of uranyl ion sorption on mesoporous silica**, Colloids Surf., A: Physicochem. Eng. Aspects 22 1 (2003) 149–162. https://doi.org/10.1016/S0927-7757(03)00139-0

Sturchio et al (1998).
Sturchio N. C., Antonio M. R., Soderholm L., Sutton S. R., Brannon J. C., **Tetravalent Uranium in Calcite,** Science 281 (1998) 971-973 doi: 10.1126/science.281.5379.971

Su et al (2018)
Su S., Che R., Liu Q., Liu J., Wang J.,
Zeolitic Imidazolate Framework-67: A promising candidate for recovery of uranium (VI) from seawater, Colloid Surf. A, 547 (2018) 73-80. https://doi.org/ 10.1016/j.colsurfa.2018.03.042

Thoenen (2000)
Thoenen T., PSI Technical Report AN-44-00-11, (2000)

Villalobos et al (2004).
Villalobos M., Trotz M.A., Leckie J.O., **Variability in goethite surface site density: Evidence from proton and carbonate sorption,** J. Coll. Interface Sci., 268 (2004) 273-87. https://doi.org/10.1016/j.jcis.2003.07.044

Ulrich et al (2006)
Ulrich K.-U., Rossberg A., Foerstendorf H., Zänker H., Scheinost A.C.,
Molecular characterization of uranium(VI) sorption complexes on iron(III)-rich acid mine water colloids.
Geochim. Cosmochim. Acta, 70 (2006) 5469-5487. https://doi.org/10.1016/j.gca.2006.08.031

Ulrich et al (2009).
Ulrich K.-U., Ilton E.S., Veeramani H., Sharp J.O., Bernier Latmani R., Schofield E.J., Bargar J.R., Giammar D.E.,
Comparative dissolution kinetics of biogenic and chemogenic uraninite under oxidizing conditions in the presence of carbonate. Geochim. Cosmochim. Acta, 73 (2009) 6065-6083. https://doi.org/10.1016/j.gca.2009.07.012

Wang et al (2015).
Wang Z., Ulrich K.-W., Pan C., Giammar D. E., **Measurement and Modeling of U(IV) Adsorption to Metal Oxide** Environmental Science & Technology 47 (2015) 850-858, https://doi.org/10.1021/acs.estlett.5b00156